Tin Bath Bottom Blocks – a Comparison of Refractories of the Systems $SiO_2 – Al_2O_3$ and $CaO – Al_2O_3$

This paper deals with the corrosion behaviour of bricks of the system $SiO_2 – Al_2O_3$ and $CaO – Al_2O_3$ against alkaline compositions of the glass as well as float atmosphere. The results show that the float atmosphere affects the calcium aluminate brick while the chamotte brick remains unaffected.

Introduction

The first production line for flat glass by the float process on the European continent was built in Köln-Porz in 1965. The then new technical procedure yielded many advantages for the production of flat glass. Meantime this process has been described extensively [1; 2; 3; 4, 5] and is well known among experts, which is why we will not discuss it in detail here.

Figure 1 shows a vertical section of a float bath to remember the construction. As can be seen, the liquid tin lies on fireclay bricks. The main producers of these bricks in Europe are *RHI* (formerly *Didier*), *P-D refractories GmbH* (formerly *VGT-DYKO*) and *DSF Refractories & Minerals Limited* (UK).

As described in the literature mentioned above, the slagging of the bricks is controlled by a diffusion process: The sodium oxide in the glass dissolves into metallic sodium in the tin and oxidizes as it diffuses into the brick by reacting with the brick's SiO_2 glassy phase. This reaction is accompanied by a reduction in brick material which is shown by the greyish colour of used bricks. The transformation leads to the formation of albite ($Na_2O \cdot Al_2O_3 \cdot 2\ SiO_2$) or nepheline ($Na_2O \cdot Al_2O_3 \cdot 6\ SiO_2$) in the contact area of liquid tin and brick material. The significant difference between the thermal expansion coefficients of nepheline and the brick material gives rise to the so-called flaking phenomena which can greatly affect the quality of flat glass production.

This was the reason to look for new refractory qualities that are not subject to this attack mechanism. Routschka has written a report about the absorption of alkaline compositions in refractory materials under tin bath bottom conditions in float glass production [6]. Strohm also reported about brick qualities resistant to alkaline compositions at the meeting of technical committees II and III of the DGG/HVG on 17–18 October 2007 in Puschwitz (*P-D refractories*, Wetro plant) [7]. The studies of Routschka were carried out at the institute of the German refractory industry in Bonn and were transferred to the industry afterwards. It took a longer development period for the industry to improve calcium aluminate bricks to technical perfection before taking this material into the production process [8].

Until now only the chemical reactions of the alkaline containing tin with the tin bath bottom blocks were studied but the influence of the float bath atmosphere on these reactions has been neglected.

In this study, the corrosion behaviour of briks of the system $SiO_2 – Al_2O_3$ and $CaO – Al_2O_3$ in the presence of alkaline compositions as well as in float atmosphere was investigated. Besides nitrogen and hydrogen the atmosphere also contains water vapour and tin sulphide as well as alkali compounds, hydrogen sulphide and elemental tin vapour.

G. Boymanns, F. Gebhardt, M. Schilling
P-D refractories GmbH DYKO-GLASS, Wiesenstr. 61, 40549 Düsseldorf, Germany

Corresponding author: M. Schilling, *michaela.schilling@pd-group.com*

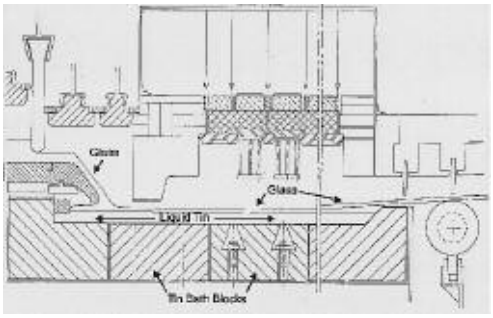

Fig 1 Vertical section of a float tank

Testing program

The properties investigated to characterize the bricks are discussed below. Table 1 shows the chemical, physical, technical and mineral data of the two brick systems.

Pore Size Distribution

The pore size distribution is very important for the absorption of smallest solid particles, liquids (smelting) and gases into refractory materials. The absorbing capacity of the mentioned materials rises with increasing pore-size values. Žagar defined the intrusion velocity of a melt into the pores of a brick as the quotient of surface tension and viscosity of the melt and named this factor capillary mobility [9]. Concerning tin bath bottom bricks Busby showed that the thermal transpiration which leads to the formation of H2 bubbles at the tin side of the glass sheet begins at a pore diameter of < 10 µm [10]. The diagram of the pore-size distribution measured in an $Al_2O_3 – SiO_2$ brick shows a bimodal configuration. The pore-size distribution of the calcium aluminate brick leads to different diagrams for the interior and exterior zone. While the interior area shows a mono modal configuration, the exterior part is more bimodal. Figure 2 gives a comparison of all curves.

Table 1 Data comparison of brick system Al_2O_3 – SiO_2 and brick system CaO – Al_2O_3

	Brick system Al_2O_3 – SiO_2		Brick system Al_2O_3 – CaO	
	Data sheet	Analysis	Data sheet	Analysis
Chemical composition / mass-%				
Al_2O_3	40	39,5	68	66,7
SiO_2	55	56,3	5	4,5
CaO		0,1	24	24,7
MgO		0,2	1,5	1,8
Na_2O		0,5		0,3
K_2O		0,6		0,1
TiO_2		1,4		
Fe_2O_3	1,2	0,9	0,1	0,15
Physico-technical properties				
Bulk density / g/cm³	21	2,1	2,36	2,4 - 2,47
Open porosity / vol.-%	23	21	18	14,2 17,1
Cold crushing strength / N/mm²	40	44	80	76 - 133
Thermal expansion at 1000 °C / %	0,65	0,63	0,65	0,68
Thermal conductivity / W/m · K at (°C)	1,44 (300)	1,63 (400)	1,3 (500)	1,95 (300)
	1,54 (500)	1,50 (600)	1,1 (750)	1,53 (600)
	1,64 (900)	1,56 (1000)	1,1 (1000)	1,45 (900)
Method of determination	hot-wire (parallel) method (DIN EN 993-15)	hot-wire (parallel) method (DIN EN 993-15)	Dr. Klasse	hot-wire (parallel) method (DIN EN 993-15)
H_2-diffusion / mm WS	≤ 150	45	30	3 - 4
Mineral data				
	no information	mullite 44 % Cristobalite 21 % quartz 6 % glassy phase 29 %	calcium aluminate	calcium dialuminite gehlenite calcium aluminate (minor phase)

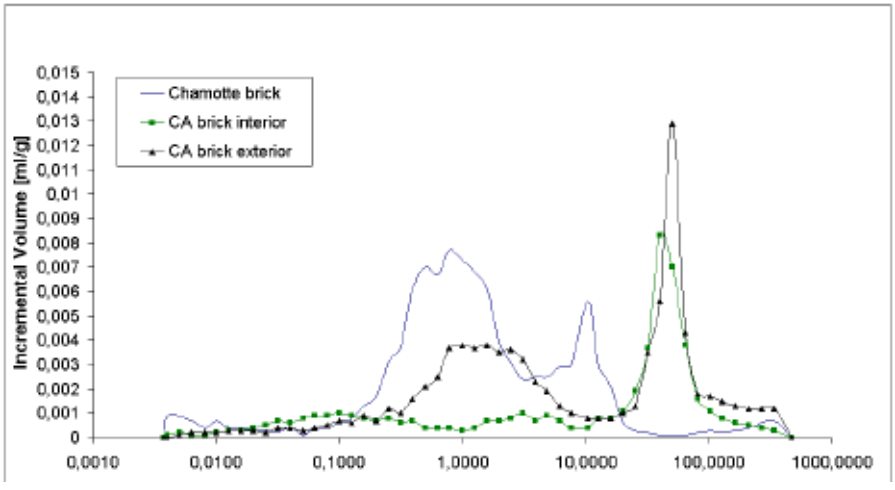

Fig 2 Comparison of pore size distribution in a fire clay brick and in a calcium aluminate brick (interior and exterior zone)

Characterization of the Tin Bath Bottom Bricks

The chemical and physical data as well as the mineral composition with the resulting texture of the chamotte bricks are well known and have been discussed in many publications which we have already mentioned.

We will therefore confine ourselves here to the characterization of the calcium aluminate bricks. One sample close to the surface and one sample of the interior of the calcium aluminate brick were investigated by microprobe analysis. Both samples show the same grain size distribution without preferred direction in a quasi dense texture. The grains are completely surrounded by the SiO_2 containing binding agent that leads to reaction seams with the calcium aluminate grains.

The MgO component appears either as grain itself or in small spaces between crystals. The ratio of MgO/Al_2O_3 is max. 0,5 [(28 – 33) % MgO / (66 – 68) % Al_2O_3 / with Fe_2O_3 (0.7 – 1,3) %]. The ratio of MgO/Al_2O_3 spinel is 0,75. However the crystals on the fracture surface are spinel. The surrounding of the spinel is formed by an Al_2O_3-CaO-SiO_2 phase which is normally the matrix.

The microstructure of both samples is uniform, but the matrix inside is denser than outside. It can be assumed that the inside part shows more closed pores than the outside part. The SiO_2 containing phase that has been identified as gehlenite by X-ray diffraction analysis forms the matrix which is better crystallised in the outside regions than inside. MgO exists in fine spinel particles which are, in contrast, finer inside than outside.

Corrosion Test

Predicting the service performance on the basis of laboratory tests is always a very complex and lengthy procedure. It presupposes that tests are conducted with different brick materials over an extended period of time under conditions which are similar as much as possible to those of the float bath. In the end the results can be compared with each other. In former times crucible tests with sodium carbonate and sodium hydroxide were supposed to show the alkali resistance of tin bath bottom bricks. But the mechanism of these reactions is quite another one than in the float bath. So in this corro-

sion test crucibles made from the different materials were filled with metallic tin that contains about 4 % metallic sodium and then treated at 1000 °C for 360 h in float atmosphere (95 % N_2 / 5 % H_2). Afterwards the crucibles were cut and the contact areas compared visually and microscopically.

Figure 3 shows the reaction area of the fireclay brick (at 50x magnification) after the test under the above mentioned conditions. A dark field projection shows dark coloured grains that clearly indicate the formation of albite and nepheline. Furthermore the decreasingly alkaline attack towards the brick interior is to be seen.

Figure 4 shows the results of the calcium aluminate brick under the same conditions. This quality has only a very small reaction area, in which metallic tin is included.

To determine the alkali content and alkali infiltration in the refractory material, microprobe analyses were carried out of the tin contact zone in the calcium aluminate brick after the described corrosion test. At two different positions in the corrosion zone the element distribution was determined and a semi quantitative analysis was carried out. The texture of the calcium aluminate brick shows three main compounds next to the tin contact zone (Table 2). The alkali infiltration can be clearly seen in the corrosion zone. During the slagging reaction the compound $2\ Na_2O \cdot 3\ CaO \cdot 5\ Al_2O_3$ ($C_3N_2A_5$) was formed. This result is in good agreement with the data given in the phase diagram $Na_2O - CaO - Al_2O_3$ (Figure 5, [11]).

The differences in the density values (ρ $CaO \cdot 2Al_2O_3$ = 2,9 g·cm^{-3}, ρ $2CaO \cdot Al_2O_3 \cdot SiO_2$ (gehlenite) = 3,04 g·cm^{-3} and ρ $2Na_2O \cdot 3CaO \cdot 5Al_2O_3$ = 2,56 g·cm^{-3} [12]) are responsible for the fine cracks in the surface layers of the calcium aluminate bricks (Fig. 6).

Tab 2 Main compounds next to the tin contact zone of the calcium aluminate brick

Compound / mass-%	Al_2O_3	Na_2O	CaO
Point 1	65	14	18
Point 2	62	17	20
$2\ Na_2O \cdot 3\ CaO \cdot 5\ Al_2O_3$ ($C_3N_2A_5$)	63	17	20

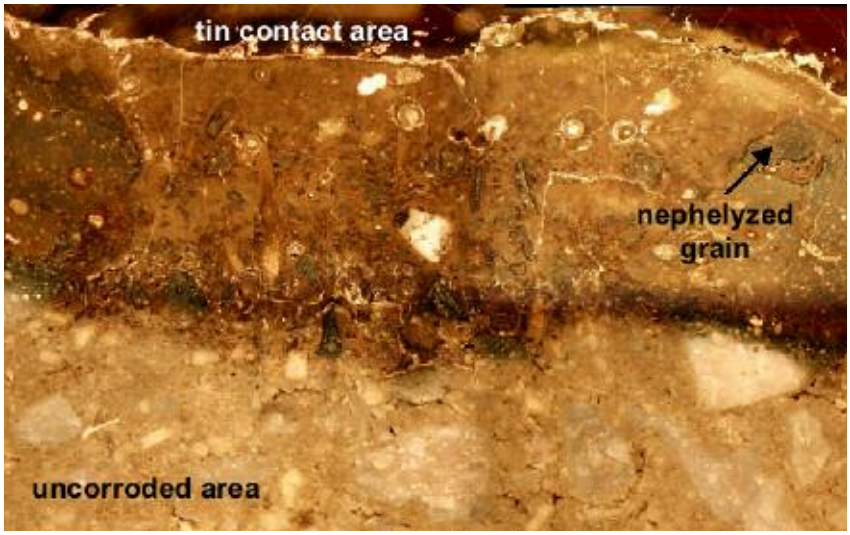

Fig 3 Dark field light microscopic image of fireclay grains with nephelitic grain boundaries taken from the contact zone of a used tin bath block

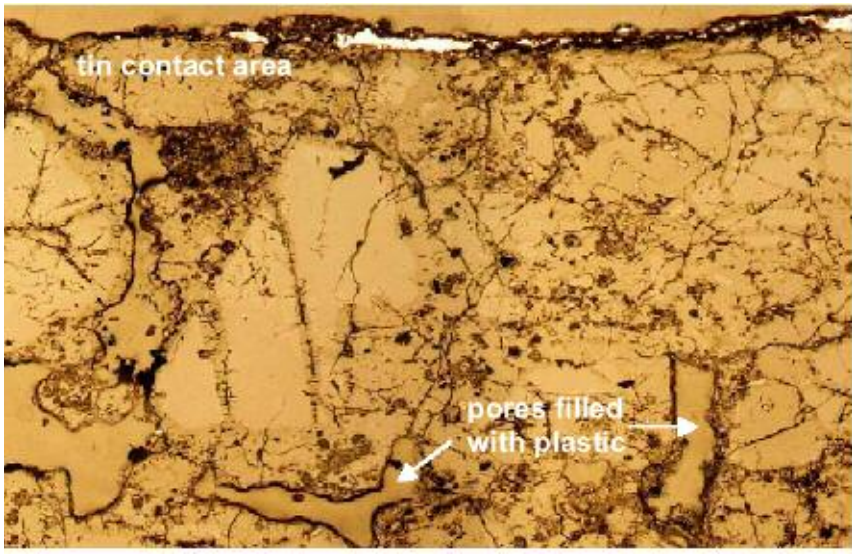

Fig 4 Light microscopic image of the corrosion zone of the calcium aluminate brick

The presence of $2Na_2O \cdot 3CaO \cdot 5Al_2O_3$ was also proved by X-ray powder diffraction analysis of a pulverized sample of the corroded zone material.

Up to now all examinations and discussions about the characteristics of tin bath bottom bricks in the float bath focused on reactions with alkali oxides. It has always been ignored that the atmosphere of the float bath – as mentioned before – not only includes nitrogen and hydrogen but also water vapour, hydrogen sulphide, sodium sulphide, tin sulphide and metallic tin. Also, the tin bath bottom bricks show a temperature gradient from the tin contact side to the bottom of the casing. This gradient changes with the thickness of the glass produced.

Thus the behaviour of calcium aluminate brick in the presence of water vapour and hydrogen sulphide has to be proved. Brick pieces and pulverized material have been treated with water vapour at different temperatures. Afterwards mineral changes were analysed by X-ray diffraction. It was noticed that the vaporized samples form calcium aluminate hexahydrate, $2CaO \cdot Al_2O_3 \cdot 6H_2O$ (ρ $CaO \cdot 2Al_2O_3$ = 2,90 g · cm^{-3}, ρ $2CaO \cdot Al_2O_3 \cdot 6H_2O$ approx. 1,95 g · cm^{-3} [13]). After drying and again heating up, the formed hydrates do not rebuild the original aggregates. Examinations

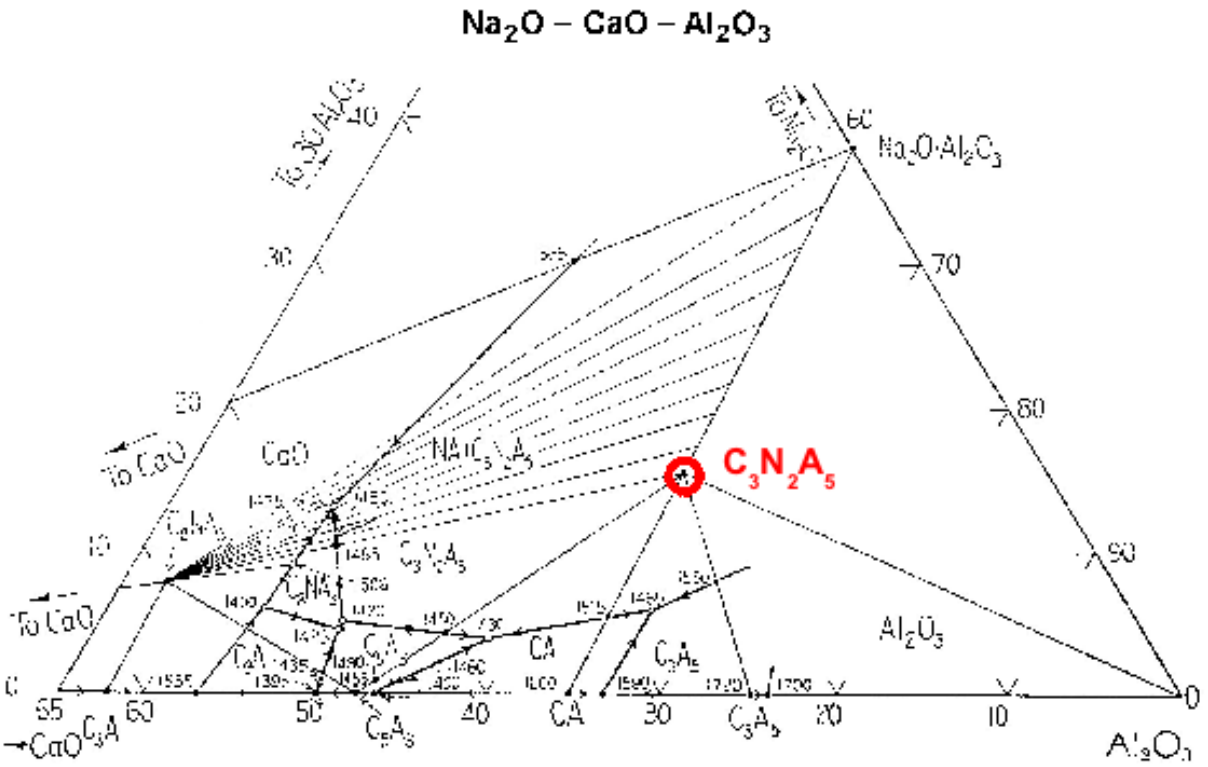

Fig 5 High aluminium corner of the phase system Na_2O - CaO - Al_2O_3

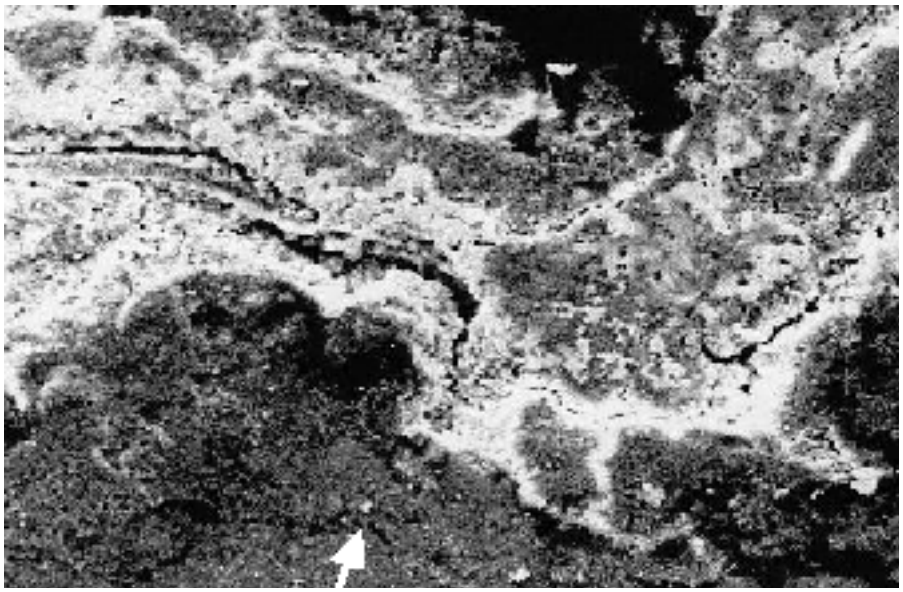

Fig 6 Reaction zone of the calcium aluminate brick after corrosion test

from Lehmann [14, 15] may perhaps give an explanation to these studies. Vaporization trials at high temperatures (900 °C, 50 h dwell time) do not show changes in the outer region of the brick.

To study the influence of the sulphide compounds in the atmosphere, the reactions in float tanks were analyzed by thermodynamic calculations of variations in the temperature and reactive quantities of protective gas and glass melt. Following the calculations the reactions of protective gas with the glass melt lead to decomposition of sodium sulphate (Na_2SO_4) in the glassy phase. Therefore a high sulphur potential is formed under strong reducing conditions in the glassy phase. The reactions of the product gases from the reaction protecting gas – glass melt with calcium dialuminate ($CaO \cdot 2Al_2O_3$) yield to the formation of more or less calcium sulphide (CaS), depending on the ratio of gas volume and glass surface. The reactions of the product gases – formed by the reciprocal action of protective gases and glass and liquid tin – reduce the partial pressure of sulphur in the float atmosphere. For the corrosion of refractory materials forming calcium sulphide, the amounts of protective gas and glass melt, which are in relationship with each other, are responsible. On the other hand this is dependent on mixtures of the steaming gas composition and their contact with liquid phases [16].

The formation of calcium sulphide (CaS) by reaction of hydrogen sulphide (H_2S) and calcium aluminate ($CaO \cdot x\,Al_2O_3$ / x = 2 and 6) has been demonstrated by thermodynamic calculations for the system glass – tin – refractory material – float atmosphere. The dialuminate, $CaO \cdot 2Al_2O_3$, reacts more strongly than the hexaaluminate, $CaO \cdot 6Al_2O_3$. The experimental confirmation is not yet complete. Both reactions, the formation of hydrates and the sulphide formation, lead to a partial phase transformation in the calcium aluminate refractory. As expected, no water vapour and sulphide forming reactions take

place in the brick system $SiO_2 - Al_2O_3$ at float tank temperatures.

Conclusion

Proceeding from the chemical analysis of the material one can see that there are great differences between the brick systems $SiO_2 - Al_2O_3$ and $CaO - Al_2O_3$. This is naturally shown in the physical data like bulk density, open porosity and especially in thermal conductivity. The high bulk density and, hence, low open porosity of calcium aluminate brick compared to chamotte brick leads to higher temperature values of calcium aluminate in the lower temperature area of the float bath, which causes stronger cooling of the casing. With increasing temperature the values of the thermal conductivity grow closer together. So the data sheet values of the calcium aluminate brick do not stand up to an international comparison with values measured using the hot-wire parallel method according to DIN EN 993-15, because they are measured by the method of Dr. Klasse. The thermal conductivity values therefore have to be corrected from the given value of 1,1 W/m · K to 1,45 W/m · K at 1000 °C. Fundamental differences are shown also in the pore size distribution, as can be seen in the diagrams. The aim of improved alkali resistance can obviously be reached with calcium aluminate bricks. But at higher magnification the microscopic analysis also shows that phase transformations take place in the contact zone, followed by horizontal microcracking.

The reaction zone of the calcium aluminate brick is much smaller than in the chamotte brick. But this zone shows a high sodium oxide enrichment of about 15 % after only a short time of testing. So the question arises what will happen by the high alkali oxide content in the brick surface during the long lifetime of the float bath.

It should be noted that the bricks adsorb water vapour in the colder temperature area and again emit this water during temperature change without rebuilding the original state. The thermodynamic calculations show the formation of calcium sulphide (CaS) over the whole temperature range of the float bath. How far the latter reactions influence the resistance of the calcium aluminate briks contrary to the chamotte bricks may be evaluated not until after a longer lifetime of a glass tank.

This survey refers to laboratory tests which are in good agreement – certainly where the chamotte qualities are concerned – with practical experience. In laboratory tests temperature conditions can be simulated close to industrial practice, but it is not possible to simulate the time factor. So what really happens will show in industrial practice.

References

[1] P. Sardjono: Chemisch-thermodynamische Untersuchung über das Verhalten von Natrium während des Floatglasprozesses. Der Fakultät für Bergbau, Hüttenwesen und Geowissenschaften der RWTH Aachen vorgelegte Dissertationsschrift 1995

[2] F.H. Hayes: Thermodynamic Considerations in the Float Glass Process. Proceedings of a Symposium held at Brunel University and National Physical Laboratory on 14th, 15th and 17th July, 1971, London, Her Majesty's Stationary Office 1972

[3] F. Müller, S.-K. Lim, F. Gebhardt, D. Küstner: Physico-chemical investigation of the behaviour of sodium in the float glass process, Part I: Distribution of sodium and tin between the glass melt and the bath of molten tin, Part II: Reactions of sodium and oxygen dissolved in the bath of molten tin. Glastechn. Ber. 62 (1989) [11] 369–376; [12] 417–421

[4] G. Routschka und F. Gebhardt: Über die Alkaliaufnahme feuerfester Werkstoffe unter den Bedingungen im Boden der Zinnbadwanne von Floatglasanlagen. Sprechsaal 127 (1994) 350–353

[5] K. Wieland, T. Weichert und G. Routschka: Zinnbadbodensteine. XXXVI. Int. Feuerfest-Kolloquium Aachen "Feuerfeste Werkstoffe in der Glasindustrie", Verlag Stahleisen (1993) 101–105

[6] G. Routschka: Abschlußbericht des AiF-Forschungsvorhabens Nr. 7427 – Reaktionsabläufe bei der Verschlackung feuerfester Werkstoffe im Floatglasprozess – am Forschungsinstitut der Feuerfest-Industrie in Bonn (1990)

[7] H. Strohm, G. Boymanns, F. Gebhardt: Refractory materials for the production of flat glass by the float process. Refractories Manual (2007)

[8] A. Eschner, T. Weichert, K. Wieland, C. Woehrmeyer: Fire resistant and refractory bricks for lining tin baths for the manufacture of float glass and their manufacture. Didier Werke AG, Deutschland – Patent: Priority Application Information DE 1993 – 4304765 A 19930217

[9] L. Žagar: Über den Einfluss der Textur auf die Verschlackungsvorgänge an feuerfesten Baustoffen. Tonind.–Ztg. (TIZ-Zbl.) 83 (1959) [6] 115–118

[10] C.M. Carr, T.S. Busby: Thermal Transpiration. Literature Review No.16 (1978) of BGIRA (British Glass Industry Research Association)

[11] E.M. Levin, C.R. Robbins and H.F. McMurdie: Phase diagrams for ceramists, Fig. 480, 174 (1964), The American Ceramic Society; L.T. Brownmiller and R.H. Bogue: Bur. Standards J. Research 8 (1932) [2] 293; R.P. 414

[12] H. Verweij: Phase Formation in the System $Na_2O \cdot Al_2O_3 - CaO \cdot Al_2O_3 - Al_2O_3$ at 1200 °C in Air. J. Am. Ceram. Soc. 69 (1986) [2] 94–98

[13] H. Freund: Handbuch der Mikroskopie in der Technik, Band IV, Teil 5, S. 159, Umschau Verlag Frankfurt am Main, 1974

[14] H. Lehmann, K.-J. Leers: Reaktionen bei der Erhärtung von Tonerdezementen. Tonind.-Ztg. 87 (1963) 29–41

[15] Salmang / Scholze: Keramik, 7. vollständig neu bearbeitete und erweiterte Auflage, herausgegeben von Rainer Telle, Springer Verlag, S. 763–767

[16] I. Barin: Reaktionen zwischen H2-N2-Schutzgas, Glasschmelze, Zinnbad und den feuerfesten Stoffen aus $CaO \cdot 2\,Al_2O_3$ und $CaO \cdot 6\,Al_2O_3$ in einer Floatglas-Anlage. Private Mitteilung